A new vorticity distribution 'blob' for generation at free surfaces

A NEW VORTICITY DISTRIBUTION 'BLOB' FOR GENERATION AT FREE SURFACES

W.W.F. Pijnappel & C.W.M. van der Geld
Eindhoven University of Technology, Faculty of Mechanical Engineering
P.O. box 513, 5600 MB Eindhoven, the Netherlands

Summary

The creation of vorticity by a uniform flow at a free interface is modelled by a new concept of vorticity distributions. The tangential stresses induced at the surface are shown to be better than that of the common 'blob'-models.

Introduction

In the past a considerable volume of numerical methods have been established coping with turbulent flows. The discrete vortex blob methods give direct physical insight in and accurately predict the development of the flow behind an obstacle. Until now these studies have been restricted to flows around solid objects [1], [2], [3]. The turbulence in the fluid is a consequence of the no-slip condition at the solid surface.
In this contribution flows around free boundaries are modeled. The creation of vorticity is then caused by tangential stresses at the free surface. The strength of the vorticity is weak and localised, which gives rise to a reexamination of the use of the well known blobs for representing localised vorticity. This is the object of this paper. Due to shortcomings of the blob model, an alternative way is suggested to circumvent the use of blobs as sources of vorticity creation. To this end a new boundary vorticity distribution is introduced.

The numerical model in short

The following modelling assumptions are made : incompressible, isothermal, two-dimensional flow around a simply connected free surface. Velocities at infinity are finite and without a component in the y-direction, in polar coordinates :

$$\Psi \sim U_\infty r \sin(\theta) \quad (r \rightarrow \infty) \tag{1}$$

The viscosity inside the bubble is very small compared with the outer fluid, and is therefore neglected. The pressure inside the bubble is assumed to be constant. The mathematical model comprises two functions, the stream function and the function describing the bubble surface. The stream function is composed of three different types of functions, as will be explained in the next subsection. One of these functions is the new vorticity distribution that is the main topic of this paper.

The stream function

The flow field is described by a stream function Ψ satisfying the Poisson equation $\nabla^2\Psi = -\omega$. Using polar coordinates, the instantaneous velocities in radial and tangential direction are

$$u_r = \frac{\partial\Psi}{r\partial\theta} \quad \wedge \quad u_\theta = -\frac{\partial\psi}{\partial r} \tag{2}$$

The stream function Ψ is split[1] into a rotational part, Ψ_{rot}, and a potential part Ψ_{pot}

$$\Psi = \Psi_{rot} + \Psi_{pot} \tag{3}$$

with

$$\nabla^2\Psi_{pot} = 0 \quad \wedge \quad \nabla^2\Psi_{rot} = -\omega \tag{4}$$

The potential part describes the flow far away from the bubble. In the vicinity of the bubble viscous effects lead to vorticity being shed from the free surface. This vorticity is modeled by Ψ_{rot}.

The harmonic function Ψ_{pot} is developed in the origin. Its domain is the unbounded fluid domain exterior of the bubble.

$$\Psi_{pot} = \sum_{n=0}^{\infty} \frac{a_n}{r^n}\cos(n\theta) + \sum_{n=0}^{\infty} \frac{b_n}{r^n}\sin(n\theta) + U_\infty r \sin(\theta) \tag{5}$$

Note that there is no vortex and no source at the origin of the coordinate system. The coefficients a_n and b_n are time-dependent.

[1] Each flow field can be uniquely described in this manner, as discussed by van der Geld [6]

At any instant of time two types of vortices prevail in the fluid : a finite number of free discrete vortices and what shall be named the boundary vorticity distributions. Discrete vortices are being used in many shapes, most of them close to the Gaussian shape [3]. They will be described first. The rather awkward application of these vortices to the boundary conditions prevailing at a free surface will be considered in some detail to facilitate comparison with the new vorticity distributions later in this paper.
The contribution to the streamfunction Ψ_{rot} of a discrete vortex at polar coordinates (r_i, θ_i) is

$$\Psi_{rot,i}(r,\theta) = -\frac{\Gamma_i}{4\pi} \ln(\sigma^2 + r^2 + r_i^2 - 2rr_i \cos(\theta - \theta_i)) \tag{6}$$

Γ_i is the strength of the vortex and σ is the core radius taken constant in time without loss of generality.
The flow field induced around a nearly spherical 2-D bubble by a discrete vortex close to a bubble and the subsequent convection experienced by the vortex are approximately described for small σ by a mirror image system consisting of three vortices. If the point P on the bubble interface closest to a discrete vortex D has curvature c and the center of curvature of P is C then vortex D is accompanied by a vortex situated on the line segment CP at distance $\frac{CP^2}{CD}$ from C with opposite strength, and a vortex at the centre C with the same strength as vortex P. Thus, every discrete vortex close to the bubble boundary is accompanied by two imaginary vortices to form a mirror image system. As long as the vorticity is already detached from the free surface, this is a satisfactory solution.
The tangential stress condition at the bubble interface, however, cannot adequately be satisfied using the above-mentioned potential function and discrete vortices. In contrast to a solid boundary, where the no-slip boundary condition can be satisfied by a vortex sheet at the boundary describing a discontinuous velocity jump, the tangential stress condition at the free surface requires continuous velocity gradients. A new boundary vorticity distribution is presented below that satisfies this and other conditions.

First the governing equations and boundary conditions are presented along with some remaining details of the numerical algorithm. The failure of the discrete blobs to satisfy the tangential stress condition is examined next, only to be followed by the presentation of the new boundary vorticity distribution (BVD).

Governing equations and numerical algorithm

The tangential stress condition at the interface reads

$$\vec{t}\mathcal{P}_{liquid}\vec{n} = \vec{t}\mathcal{P}_{gas}\vec{n} \tag{7}$$

Here $\mathcal{P}$ is the stress tensor, $\vec{n}$ is the normal unit vector, pointing into the fluid and $\vec{t}$ is the tangential unit vector.

$$\vec{t}\mathcal{P}\vec{n} = \eta\left(\left(\omega + 2\frac{\partial^2\Psi}{\partial r^2}\right)(t_r^2 - n_\theta^2) + 4\frac{\partial}{\partial r}\left(\frac{\partial\Psi}{r\partial\theta}\right)n_r n_\theta\right) \tag{8}$$

At every timestep a new boundary vorticity distribution is computed with the help of this tangential stress condition.
The potential part of the streamfunction is calculated by examining the evolution of the pressure along contours which intersect the bubble boundary twice.
The pressure drop between two points in the liquid is calculated by integrating the Navier Stokes equation

$$\rho\frac{D\vec{u}}{Dt} = \rho\vec{g} - \nabla p + \eta\nabla^2\vec{u} \tag{9}$$

The only unknowns are the time derivatives of all coefficients a_n and b_n in Ψ_{pot}. Due to the curvature of the surface of the bubble the surface interface shows a pressure jump given by the normal stress condition:

$$\vec{n}\mathcal{P}_{gas}\vec{n} - \vec{n}\mathcal{P}_{liquid}\vec{n} = \frac{\gamma}{r_c} \tag{10}$$

Here r_c is the radius of curvature and γ is the surface tension coefficient. The integrated Navier Stokes equations and the normal stress conditions along a closed contour which intersect the interface twice sum up the zero total pressure drop which yields an equation in the unknowns $\frac{\partial a_n}{\partial t}$ and $\frac{\partial b_n}{\partial t}$. Several of these equations, each corresponding to a different contour, are put together in a matrix that is solved for the unknowns. This procedure has more detailedly been described by [6].

The bubble radius R is supposed to be a single-valued function of the angle θ. The function $R(\theta)$ is expanded in a Fourier series. The bubble shape is calculated at each timestep by a least squares cubic splines fit using the kinematic boundary condition, that reads

$$\frac{\partial R(\theta)}{\partial t} = u_r - u_\theta\frac{\partial R}{R\partial\theta} \tag{11}$$

Time-integration of this equation with the Adams-Bashford method yields the time evolution of the surface.

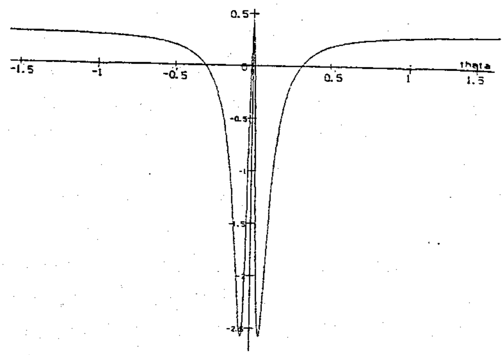

Figure 1: Tangential stress induced on the free interface of a circular bubble with radius 1 mm. by a mirror image system with $\sigma = 0.05$ mm.

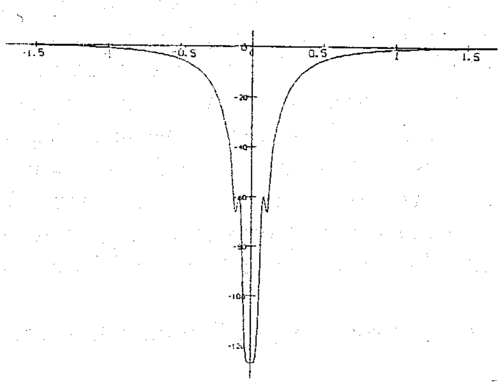

Figure 2: Tangential stress induced on the free interface of a circular bubble with radius 1 mm. by a single BVD with $\alpha = 10$

The discrete blobs attempt

There is a simple way to satisfy the tangential stress condition at a discrete set of points on the bubble surface. Newly created discrete vortices are put at so-called 'creation point' away from the bubble interface, possibly extended to mirror image systems as described above. The strengths of these vortices are calculated from the tangential stress condition.
The resulting strengths of these vortices turn out to be strongly dependent on the distance between the creation points and the interface. They are also that large, that the bubble experiences irrealistic forces at its boundary as demonstrated below. The main problem seems to be that the vorticity in this method is created at a distance from the interface.
E.g., consider a circular 2-D bubble of radius 1 mm, and a system of three vortices. One of strength 1 s^{-1} at a distance of 1.05 mm from the center of the bubble. One mirror vortex of strength -1 at a distance of 1/1.05 mm from the centre, and one vortex of strength 1 in the center of the bubble. The tangential stress induced on the free interface by this mirror image system is shown in Fig. 1 for vortices with core radius $\sigma = 0.05$ mm. If the core radius does not exceed 0.016787 the tangential stress plot exhibits only one peak.
Now add a uniform flow of 0.1 m/s; the streamfunction is $\Psi = -\frac{100}{r}\sin(\theta)$; the number of creation points is 40 and the creation points are placed at equal distances, 1.05 mm from the center of the bubble. If the core radius is $\sigma = 0.016787$ the tangential stress induced on the surface by the potential flow plus the vortices at the creation points and their images is as shown in Fig. 3. It is a curve enclosed by an enveloping sine and the θ-axis. This characteristic is also exhibited for other values of σ. E.g. for $\sigma = 0.05$ the tangential stress varies between -243 and 243; for $\sigma = 0$ between -90 and 90. For $\sigma = 0.02252$ the variation is minimal, between -12 and 12.
For $\sigma = 0.05$ the created vortices have strengths between -128.7 and 128.7, for $sigma = 0.02252$ between -44.3 and 44.3 and for $\sigma = 0$ between -24.5 and 24.5.
The strength of the new vorticity distribution will be seen to be of order one.

The New Boundary Vorticity Distribution

During a timestep Δt the vorticity that is created at the free surface smears out. Let us assume that after Δt the new vorticity distribution can be conveniently be described as having a strength inversely proportional to some power of the distance to the center of local surface curvature, as defined below. This will lead to the new boundary vorticity distribution (BVD) introduced in this section.
Select a finite number p of so-called 'pivotal points', representative of the interface. This can be achieved if the surface is split up into a finite number

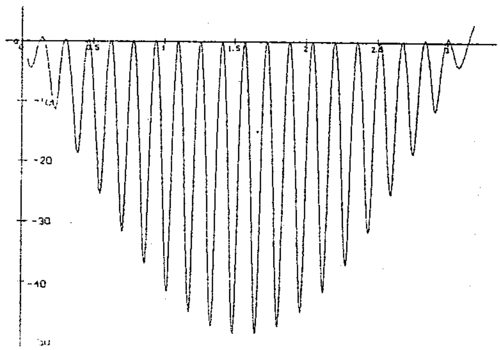

Figure 3: Tangential stress induced on the free interface of a circular bubble with radius 1 mm. by a complete mirror image system with 40 creation points and $\sigma = 0.016787$

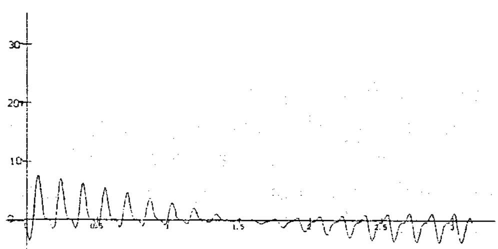

Figure 4: Tangential stress induced on the free interface of a circular bubble with radius 1 mm. by a complete BVD envelop and $\alpha = 10$

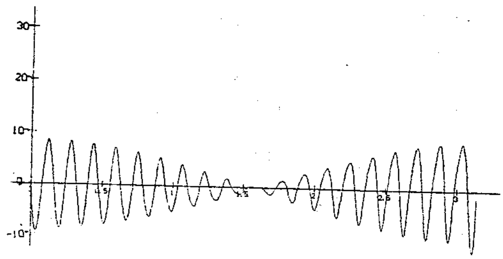

Figure 5: Tangential stress induced on the free interface of a circular bubble with radius 1 mm. by a complete BVD envelop and $\alpha = 40$

p of circular arcs. The pivotal points are the midpoints of the arcs and lie on the bubble surface. To each pivotal point with its associated arc correspond a center of curvature, M, and a half-cone C defined as the interior of the area enclosed by two semi-infinite lines. These lines start from M, the vertex of the half-cone and each goes through an endpoint of the circular arc with radius of curvature r_c. Within the half-cone C the vorticity distribution function ω is taken constant at constant distances to M. ω is zero inside the bubble and in the exterior of the half-cone.
Outside the bubble but within the half-cone boundary

$$\omega = c\Gamma r^{\alpha+2} \tag{12}$$

Here r is the distance from a point to M. With ones value of c, the total circulation induced by the cone is given by Γ, which is unknown beforehand. In the power α is a constant,e.g. $\alpha = 10$. Let ϕ_2 be the angle between the semi-infinite lines bordering the cone, then c is a normalization constant satisfying:

$$c = \frac{\alpha r_c^\alpha}{2\phi_2} \tag{13}$$

The velocities induced by this BVD is calculated with the Biot-Savart law. For a half-cone, symmetric in the positive x-axis, with the vertex in the origin, the radial velocity component u_r is

$$u_r = \frac{\alpha}{8\pi\phi R}\frac{r_c{}^\alpha}{R}\left(f(\theta-\phi) - f(\theta+\phi)\right) \tag{14}$$

with $\phi = \phi_2/2$ and

$$f(\tau) \quad = \quad \sin(\alpha\tau)\arctan\left(\frac{r_c - R\cos(\tau)}{R\sin(\tau)}\right) - \frac{\pi}{2}\sin(\alpha\tau)\,\mathrm{signum}(\sin(\tau))$$

$$
- \cos(\alpha\tau)\ln(r_c) - \frac{1}{2}\left\{\left(\frac{R}{r_c}\right)^{\alpha} - \cos(\alpha\tau)\right\}\ln(r_c^2
$$

$$
+ R^2 - 2r_cR\cos(\tau)) + \sum_{i=1}^{i=\alpha-1}\frac{\cos(i\tau)}{\alpha - i}\left(\frac{R}{r_c}\right)^{\alpha-i} \tag{15}
$$

With the use of these formulae and the continuity equation all induced velocity components and their derivatives are computed. These velocities are required for the contour integrations to determine $\frac{\partial a_n}{\partial t}$ and $\frac{\partial b_n}{\partial t}$. For example, Fig. 2 shows the tangential stress at the interface for a single boundary vorticity distribution with its vertex in the center and the half-cone symmetric in the x-axis. The cone angle is $\phi_2 = \frac{2\pi}{40}$ and the strength is 1 $s^(- 1)$. The striking difference in amplitude between the tangential stress induced by a mirror image system and a BVD is not surprising if one considers that the latter vorticity is primarily created at the bubble interface and not away from the interface. The further the creation point is put from the interface, the larger the strength of the free vortex must be to obtain the same induced tangential stress at the interface.

Fig. 4 and Fig. 5 show the residual tangential surface stress for a system of 40 BVD's equally spread around the circular bubble, so with $\phi_2 = \frac{2\pi}{40}$. In Fig. 4 $\alpha = 10$ and in Fig. 5 $\alpha = 40$. As might be expected the residual stresses caused by boundary distributions are much smaller than for free vortices. An increase in the value of α does not lead to a further a decrease in the residue. The strengths of BVD's with $\alpha = 10$ lay between -1.5 and 1.5.

The vorticity ω created at the interface should approximately satisfy the following equation [8].

$$
\omega = \frac{2U}{r_c} \tag{16}
$$

where U represents $\left|\frac{\partial\Psi_{pot}}{r\partial\theta} + \frac{\partial\Psi_{pot}}{\partial r}\right|$ and r_c is the radius of curvature once again. Using $\alpha = 10$ in the preceding example $\frac{\omega r_c}{2U} = 1.000737$ for all points at the interface. This is in good agreement with the theoretic prediction.

Transport away from the free surface

One of the main reasons for the introduction of discrete vortices is to simulate transportation of vorticity by the flow. Therefore after each timestep the BVD's are translated into discrete vortices, which are not tied to a fixed place. The convection of the discrete vortices is simulated using the Biot-Savart law. Ogami and Akamatsu [4] have shown that the diffusion can be simulated using the what they call Diffusion Velocity Method. The effect of their diffusion technique is visible in the long run. Without the diffusion the vortex blobs incline to stay closer together.

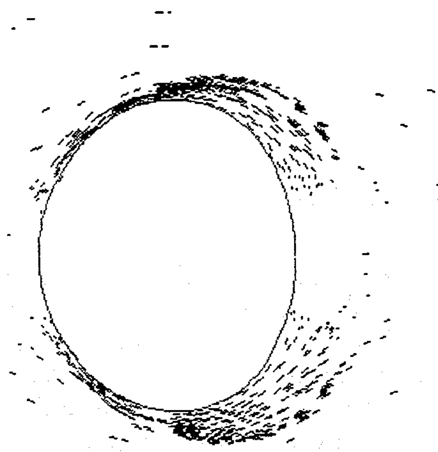

Figure 6: Wake flow and bubble deformation by a uniform flow of water of 100 mm/s past an airbubble of 2 mm in diameter

Testcases

The numerical algorithm has been subjected to several tests. The oscillatory behaviour of the interface in a potential flow corresponds with theoretical predictions [5] and the transformation of a big bubbles with a diameter larger than 20 mm. agrees with results of Walters and Davidson [7]. Consider next an air bubble floating in a uniform water flow of 100 mm/s. The bubble surface is covered with 40 BVD's. The distance of the creation points are at a distance of 0.05 mm from the interface and the core radius is 0.05 mm. In Figure 3 the fluid flow is plotted after 0.03 s. The timestep was 1.0e-4 s. These results are promising although further computations are necessary for full testing.

Conclusions

The concept of fixed creation points at which vorticity is created does not satisfy the requirements. The strengths of the vortices are strongly dependent on the distance of the creation points from the interface and are in all cases too large, causing an unstable interface.
A new concept of boundary vorticity was introduced. The stress created at the interface are in good agreement with theoretical predictions and the created vorticity is small as it should. The new boundary vorticity model can be incorporated into existing models [6]

References

[1] CHORIN, AJ, - Numerical study of slightly viscous flow, *J. Fluid Mech.*, 57, 785-796, (1973).

[2] HUNT, B - *The Panel Method for Subsonic Aerodynamic Flows: A Survey of Mathematical Formulations and Numerical Models and an Outline of the New British Aerospace Scheme*, Von Karmen Inst. for Fluid Dynamics, Lecture Series, No. 4, (1978).

[3] LEWIS, RI - Vortex *Element Methods for Fluid Dynamic Analysis of Engineering Systems*, Cambridge Engine Technology Series, (1991).

[4] OGAMI, Y, AKAMATSU, T - Viscous Flow Simulation Using the Discrete Vortex Model-The Diffusion Velocity Method, *Computers and Fluids*, Vol. 19, No 3/4, 433-441 (1991).

[5] KLOET, AM - *A Model of a Moving and Deforming 2-D Bubble Using the Discrete Vortex Method,* graduate report (1994).

[6] GELD, CWM VAN DER - *On the direct simulation of vortex shedding,* Report LR-513, Report PML 1987-C17, SFCC Publication No. 40, (1989).

[7] WALTERS, JK AND DAVIDSON, JF - The initial motion of a gas bubble formed in an inviscid liquid, *Journal of Fluid Mechanics*, vol 12, part 3, 408-417, (1961).

[8] BATCHELOR, GK - *An Introduction to Fluid Dynamics*, Cambridge University Press, (1970).